Songklanakarin J. Sci. Technol.
44 (2), 370-380, Mar. - Apr. 2022

http://www.sjst.psu.ac.th

Original Article

Convective flow and temperature distribution in rotating inclined composite porous and fluid layers

Karuna Sree Chitturi[1*], Sri Ramachandra Murty P.[2], and Sobhan Babu K.[3]

[1] *Division of Mathematics, Department of Science and Humanities, Vignan's Foundation for Science, Technology and Research, Vadlamudi, Andhra Pradesh, 522213 India*

[2] *Department of Mathematics, GIS, Gitam* (*Deemed to be University*), *Visakhapatnam, Andhra Pradesh, 530045 India*

[3] *Department of Mathematics, University College of Engineering* (*Narasaraopet*), *Jawaharlal Nehru Technological University, Kakinada, Andhra Pradesh, 533003 India*

Received: 27 July 2019; Revised: 22 July 2021; Accepted: 16 September 2021

Abstract

Convective flow and temperature distribution in rotating inclined composite porous and fluid layers, in which the pressure gradient is kept constant, is analytically studied. The fluids in all the domains are distinct in thermal conductivities, viscosities and densities. The flow is assumed to be steady, two dimensional, laminar and fully developed. Due to the inclusion of buoyancy forces, viscous and Darcy dissipation terms, the governing equations are non-linear and coupled. The solutions for region II are obtained by the regular Perturbation process, whereas the solutions for region I and region III are obtained by solving them as linear differential equations with constant coefficients. The outcomes of the governing parameters on the fluid flow are numerically computed and graphically depicted and inspected in detail. It is observed that increase in Coriolis force incorporated through the porous and rotation parameters reduces the temperature and axial velocity of fluid in the three regions.

Keywords: convective flow, inclined, rotating, composite, porous, fluid layers

1. Introduction

Many recent studies contributed to the subject of convection in a permeable medium owing to its enormous practical engineering and scientific applications such as, drying technology, energy accumulator devices, and packed-bed heat exchangers, nuclear waste respiratory and geo-thermal devices. Fluid flow is also a normal phenomenon within a revolving structure. The velocity, density, volume, etc, will have an effect on the fluid particles internally and rise as the fluid rotates. Fluid rotation can be limited, but cannot be disregarded. Flow in a revolving system has ample industrial and technical applications. One fluid occupying the entire closure case was studied in most of the existing research. The fluid mechanism also requires duo or more distinct immiscible fluids and sheets of one liquid over another layer in practical conditions. During composition and execution of fluid models in low gravity areas, the behavior of two fluid flow is of great use. Even a multilayered fluid arrangement gives a modified model for growing high quality crystals which involve the buoyancy-driven convective process. Perception of the convective interaction of composite porous and fluid layers requires modeling of such systems. Various problems in two phase flow considering porous and rotation parameter have been studied by researchers like Bian, Vasseur, Bilgen, & Meng (1996), Chauhan and Rema Jain (2005), Hadidi and Bennacer (2016), Karuna Sree Chitturi, Sri Ramachandra Murty Paramsetti, & SobhanBabu (2020). Malashetty, Umavathi, and Pratap Kumar (2001), Malashetty *et al*. (2004), Simon Daniel, & Shagaiya (2013) and Sri Ramachandra Murty, Balaji Prakash & Karuna Sree (2018). Umavathi (2005) investigated the effect of composite couple stress fluid and viscous fluids. Velocity and

*Corresponding author
Email address: karuna637@gmail.com

temperature effects in an inclined channel of composite fluid layer and porous layers was analysed by Malashetty (2005). The unsteady flow and heat transfer of porous fluid between viscous fluids were studied by Umavathi (2010). Rashidi (2012) studied chemically reacting combined heat and mass transfer effects along a horizontal surface. Kalili (2015) analyzed unsteady convective heat and mass transfer of a power-law pseudo plastic nanofluid on a stretching wall. Armaghani (2016) analyzed numerically, heat transfer and entropy generation in a baffled L-shaped cavity of water-alumina nanofluid. Mohebbi (2017) analyzed numerical simulation of natural convective flow of a nanofluid in an L-shaped enclosure having an internal heating obstacle. Also Mohebbi (2018) investigated numerical simulation of forced convection of three different nanofluids in expanded surfaces. Recently, Lu (2018) studied flow and temperature characteristics of nano fluid between two clear fluids. The peristaltic propulsion of nanofluid through a porous rectangular duct was studied by Riaz (2019) and peristaltic fow of nano particles through a curved channel with second-order partial slip and porous medium was investigated by Riaz (2020). Houman (2020) studied numerical modeling of nanoparticle migration with effects of shape of particles and magnetic field inside a porous enclosure. Zeeshan (2020) analysed nonspherical nanoparticles in electromagnet hydrodynamics of nanofluids through a porous medium between eccentric cylinders. Unsteady flow of two incompressible Maxwell fluids between infinite horizontal parallel plates in a porous medium is studied by Constantin (2021). Even though the study on convective flow and temperature distribution through composite porous and fluid layers with inclined geometry is of use, particularly in geophysical systems, there appears to be a very limited number of researchers, notably, Malashetty, Umavathi, and Kumar (2005), Umavathi, Liu, Kumar and Meera (2010), Sheikholeslami and Ganji (2014) and Lu, Farooq, Hayat, Rashidi and Ramzan (2018). The aim of the present paper is to study the effect of the parameters such as inclination angle, rotation parameter and porous parameter etc., on MHD convective flow and heat transfer through an inclined rotating system of composite fluid and porous layers.

2. Materials and Methods

The physical representation of the problem is shown in Figure 1. It is composed of two plates which are inclined, parallel and infinite in length along x and z-directions. The upper and lower plate temperatures, T_{w_1} and T_{w_2} are kept constant. 'Φ' is the angle made by the inclined channel with the horizontal plane. The regions I and III with $-h \le y \le 0$ and $h \le y \le 2h$ are loaded with clear viscous fluid with viscosity μ_1, density ρ_1 and thermal conductivity K_1. The region II with $0 \le y \le h$ is filled with porous material of permeability k, saturated with viscous fluid of density ρ_2, viscosity μ_2 and thermal conductivity K_2. The permeable medium is considered to be homogeneous and isotropic. The three fluids have constant transport properties with laminar flow, fully developed and are assumed to be in a steady state. The flow in the channel is navigated by temperature gradient $\Delta T = T_{w_1} - T_{w_2}$ and pressure gradient $\left(\frac{-\partial p}{\partial x}\right)$ which is constant and is not affected by the existence of heat transfer. When rotated with an angular velocity, mathematically the problem involves the coupling of Navier-Stokes equation (for fluid region) with Brinkman-extended Darcy equation (for porous medium) with the corresponding conditions at the common boundary of the fluid and porous layer. In order to get realistic predictions, we have considered Brinkman extended Darcy-Lapwood model. The entire system is rotated with the angular velocity Ω, about the y-axis. Therefore, for Boussinesq fluids the equations of motion and energy following Malashetty, Umavathi, and Kumar (2005) are:

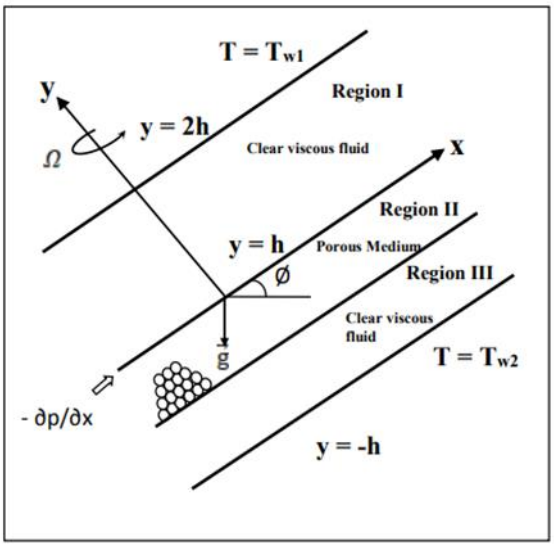

Figure 1. Physical configuration

Region-I

$$\mu_1 \frac{d^2 u_1}{dy^2} + \sin\phi\left(T_1 - T_{w_2}\right)\rho_1 g \beta_1 = 2\rho_1 \Omega w_1 + \frac{\partial p}{\partial x} \tag{1}$$

$$\mu_1 \frac{d^2 w_1}{dy^2} = -2\Omega u_1 \rho_1 \tag{2}$$

$$\frac{d^2 T_1}{dy^2} = 0 \tag{3}$$

Region-II

$$\mu_2 \frac{d^2u_2}{dy^2} + \sin\phi\left(T_2 - T_{w_2}\right)\rho_2 g\beta_2 - \frac{\mu_2}{k}u_2 = 2\rho_2\Omega w_2 + \frac{\partial p}{\partial x} \tag{4}$$

$$\mu_2 \frac{d^2w_2}{dy^2} - \frac{\mu_2}{k}w_2 = -2\rho_2\Omega u_2 \tag{5}$$

$$\frac{d^2T_2}{dy^2} + \frac{\mu_2}{K_2 k}\left(u_2{}^2 + w_2{}^2\right) = 0 \tag{6}$$

Region-III

$$\mu_1 \frac{d^2u_3}{dy^2} + \rho_1 g\beta_1 \sin\phi\left(T_3 - T_{w_2}\right) = \frac{\partial p}{\partial x} + 2\rho_1\Omega w_3 \tag{7}$$

$$\mu_1 \frac{d^2w_3}{dy^2} = -2\rho_1\Omega u_3 \tag{8}$$

$$\frac{d^2T_3}{dy^2} = 0 \tag{9}$$

where u_i and w_i are the x and z components of fluid velocity, where the subscripts i = 1, 2, 3 represents I, II, III phase values respectively. The thermal expansion coefficient is β_i and T_i is the temperature. The velocity vanishes at the walls, because of the no-slip condition. Considering the above conditions, the respective boundary and interface conditions on velocity and temperature distributions are:

$$u_1(2h) = 0,\ w_1(2h) = 0;\ u_1(h) = u_2(h),\ w_1(h) = w_2(h);\ u_2(0) = u_3(0),$$
$$w_2(0) = w_3(0)\,u_3(-h) = 0,\ w_2(-h) = 0 \tag{10}$$

$$\mu_1 \frac{du_1}{dy} = \mu_2 \frac{du_2}{dy} \quad \text{and} \quad \mu_1 \frac{dw_1}{dy} = \mu_2 \frac{dw_2}{dy} \quad at\ y = h\,, \quad \mu_2 \frac{du_2}{dy} = \mu_1 \frac{du_3}{dy}$$

$$\text{and} \quad \mu_2 \frac{dw_2}{dy} = \mu_1 \frac{dw_3}{dy} \quad at\ y = 0 \tag{11}$$

$$T_1(2h) = T_{w1},\ T_1(h) = T_2(h),\ T_2(0) = T_3(0),\ T_2(-h) = T_{w2},$$

$$K_1 \frac{dT_1}{dy} = K_2 \frac{dT_2}{dy} \ at\ y = 0\, and\, K_2 \frac{dT_2}{dy} = K_1 \frac{dT_3}{dy} \ at\ y = 0 \tag{12}$$

We have , $\frac{u_1}{u_1} = u_1^*$, $\frac{u_2}{u_1} = u_2^*$, $\frac{u_3}{u_1} = u_3^*$, $\frac{w_1}{u_1} = w_1^*$, $\frac{w_2}{u_1} = w_2^*$, $\frac{w_3}{u_1} = w_3^*$, $\frac{y_1}{h_1} = y_1^*, \frac{y_2}{h_1} = y_2^*, \frac{y_3}{h_1} = y_3^*$, $\frac{\mu_1}{\mu_2} = m$,

$$\mathrm{Pr} = \frac{\mu_1 C_p}{K_1},\ \lambda = \frac{h_2}{\sqrt{k}},\ \mathrm{Re} = \frac{\bar{u}_1 h_1}{\nu_1},\ K = \frac{K_1}{K_2},\ h = \frac{h_2}{h_1},\ n = \frac{\rho_1}{\rho_2},\ b = \frac{\beta_1}{\beta_2},\ \mathrm{R}^2 = \frac{\Omega h_1^2}{\nu_1},$$

$$Ec = \frac{\bar{u}_1^{\,2}}{C_p(T_{w1} - T_{w2})},\ \left[\frac{(T - T_{w2})}{(T_{w1} - T_{w2})}\right] = \theta,\ Gr = \frac{g\,\beta_1 h_1{}^3 (T_{w1} - T_{w2})}{\nu_1{}^2},\ P = \left(\frac{h_1{}^2}{\mu_1 \bar{u}_1}\right)\left(\frac{\partial p}{\partial x}\right).$$

Here average velocity is indicated by $\bar{u}_1$.

Applying the above transformations, the equations (1 to 9) transform to:

Region-I

$$\frac{d^2u_1}{dy^2} + \frac{Gr}{Re}(Sin\phi)\theta_1 = P + 2R^2 w_1 \tag{13}$$

$$\frac{d^2w_1}{dy^2} = -2R^2 u_1 \tag{14}$$

$$\frac{d^2\theta_1}{dy^2} = 0 \tag{15}$$

Region-II

$$\frac{d^2u_2}{dy^2} + \frac{mGr}{nb\,\mathrm{Re}}(Sin\phi)\theta_2 - \frac{\lambda^2 u_2}{h^2} = mP + 2R^2 w_2 \tag{16}$$

$$\frac{d^2w_2}{dy^2} - \frac{\lambda^2 w_2}{h^2} = -2R^2 u_2 \tag{17}$$

$$\frac{d^2\theta_2}{dy^2} + \mathrm{Pr}\,Ec\frac{\lambda^2}{h^2}\frac{K}{m}(u_2{}^2 + w_2{}^2) = 0 \tag{18}$$

Region-III

$$\frac{d^2u_3}{dy^2} + \frac{Gr}{Re}(Sin\phi)\theta_3 = P + 2R^2 w_3 \tag{19}$$

$$\frac{d^2w_3}{dy^2} = -2R^2 u_3 \tag{20}$$

$$\frac{d^2\theta_3}{dy^2} = 0 \tag{21}$$

The dimensionless forms of the interface and boundary conditions are:

$$u_1(1+h) = 0,\quad w_1(1+h) = 0,\quad u_1(h) = u_2(h),\quad w_1(h) = w_2(h),$$

$$u_2(0) = u_3(0),\quad w_2(0) = w_3(0),\quad u_3(-1) = 0,\quad w_3(-1) = 0,$$

$$m\frac{du_1}{dy} = \frac{du_2}{dy} \text{ and } m\frac{dw_1}{dy} = \frac{dw_2}{dy} \text{ at y = h,}$$

$$\frac{du_2}{dy} = m\frac{du_3}{dy} \text{ and } \frac{dw_2}{dy} = m\frac{dw_3}{dy} \text{ at y = 0,}$$

$$\theta_1(1+h) = 1,\ \theta_1(h) = \theta_2(h),\ \theta_2(0) = \theta_3(0), \theta_3(-1) = 0,$$

$$K\frac{d\theta_1}{dy} = \frac{d\theta_2}{dy} \ \ at\ \ y = h\ ,\ \frac{d\theta_2}{dy} = K\frac{d\theta_3}{dy} \ \ at\ \ y = 0. \tag{22}$$

Considering $q_1 = u_1 + i\,\omega_1$, $q_{2i} = u_{2i} + i\,\omega_{2i}$ for i = 0, 1 and $q_3 = u_3 + i\,\omega_3$, equations (13 to 21) in complex form are:

Region-I

$$\frac{d^2q_1}{dy^2} + \frac{Gr}{\mathrm{Re}}(\sin\varphi)\theta_1 = P - 2i\,R^2 q_1 \tag{23}$$

$$\frac{d^2\theta_1}{dy^2} = 0. \tag{24}$$

Region-II

$$\frac{d^2q_2}{dy^2} + \frac{mGr}{nb\,\mathrm{Re}}(\sin\varphi)\theta_2 - \frac{\lambda^2}{h^2}q_2 = mP - 2i\,R^2 q_2, \tag{25}$$

$$\frac{d^2\theta_2}{dy^2} + \mathrm{Pr}\,Ec\frac{K}{m}\frac{\lambda^2}{h^2}(q_2\,\bar{q}_2) = 0 \tag{26}$$

Region-III

$$\frac{d^2q_3}{dy^2} + \frac{Gr}{\mathrm{Re}}(\sin\varphi)\theta_3 = P - 2i\,R^2 q_3 \tag{27}$$

$$\frac{d^2\theta_3}{dy^2} = 0. \tag{28}$$

$\bar{q}_2$ is the complex conjugate of q_2.

The respective boundary and interface conditions are:

$$q_1(2)=0, q_1(1)=q_2(1), q_2(0)=q_3(0),\ q_3(-1)=0,$$
$$\frac{dq_1}{dy}=\frac{1}{m}\frac{dq_2}{dy} \quad at\ y=1,\ \frac{dq_2}{dy}=m\frac{dq_3}{dy} \quad at\ y=0 \tag{29}$$

$$\theta_1(2)=1,\ \theta_1(1)=\theta_2(1),\ \theta_2(0)=\theta_3(0), \theta_3(-1)=0,$$
$$\frac{d\theta_1}{dy}=\frac{1}{K}\frac{d\theta_2}{dy}\ at\ y=1\ ,\ \frac{d\theta_2}{dy}=K\frac{d\theta_3}{dy}\ at\ y=0. \tag{30}$$

2.1 Solutions of the problem

The governing energy and momentum equations for Region I and III are linear ordinary differential equations. Hence the solutions can be obtained using the methods of ordinary differential equations. The equations for Region I and III are

Region I

$$\frac{d^2q_1}{dy^2}+\frac{Gr}{\mathrm{Re}}(\sin\varphi)\theta_1=P-2iR^2q_1 \tag{31}$$

$$\frac{d^2\theta_1}{dy^2}=0 \tag{32}$$

Region III

$$\frac{d^2q_3}{dy^2}+\frac{Gr}{\mathrm{Re}}(\sin\varphi)\theta_3=P-2iR^2q_3 \tag{33}$$

$$\frac{d^2\theta_3}{dy^2}=0 \tag{34}$$

For Region II the governing energy and momentum equations are non-linear and coupled, so regular Perturbation Method is applied to obtain approximate solution. The perturbation parameter ε = Pr.Ec (which is small), is used as the perturbation quantity. The solutions for Region II are considered as

$$(q_i,\theta_i)=(q_{i0},\theta_{i0})+\varepsilon(q_{i1},\theta_{i1})+..... \tag{35}$$

where q_{i0},θ_{i0} are the solutions for the case when ε = 0 and $q_{i1},\theta_{i1}$are perturbed quantities related to q_{i0},θ_{i0} respectively. Substituting the above solutions in equations (25) and (26) and equating the factors of identical existing powers of ε, we obtain equations of zeroth-order and first-order approximations for Region II as follows:

Region-II

Equations of zero[th]-order approximation

$$\frac{d^2q_{20}}{dy^2}+\frac{mGr}{nb\,\mathrm{Re}}(\sin\varphi)\theta_{20}-\frac{\lambda^2}{h^2}q_{20}=mP-2iR^2q_{20} \tag{36}$$

$$\frac{d^2\theta_1}{dy^2}=0 \tag{37}$$

Equations of first-order approximation

$$\frac{d^2q_{21}}{dy^2}+\frac{mGr}{nb\,\mathrm{Re}}(\sin\varphi)\theta_{21}-\frac{\lambda^2}{h^2}q_{21}=mP-2iR^2q_{21}, \tag{38}$$

$$\frac{d^2\theta_{21}}{dy^2}+\frac{K}{m}\frac{\lambda^2}{h^2}(q_{20}\,\overline{q_{20}})=0 \tag{39}$$

Boundary conditions

$$q_1(2)=0, q_1(1)=q_{20}(1), q_{21}(1)=0, q_{20}(0)=q_3(0),\ q_{21}(0)=0,$$
$$q_3(-1)=0, \frac{dq_1}{dy}=\frac{1}{m}\frac{dq_{20}}{dy} \quad at\ y=1, \frac{dq_{21}}{dy}=0 \quad at\ y=1\ ,$$

$$\frac{dq_{20}}{dy} = m\frac{dq_3}{dy} \text{ at } y=0,\ \frac{dq_{21}}{dy} = 0 \text{ at } y=0. \tag{40}$$

$$\theta_1(2)=1,\ \theta_1(1)=\theta_{20}(1),\ \theta_{21}(1)=0,\quad \theta_{20}(0)=\theta_3(0),$$
$$\theta_{21}(0)=0,\quad \theta_3(-1)=0,$$
$$K\frac{d\theta_1}{dy} = \frac{d\theta_{20}}{dy} \quad at\ y=h=1,\ \frac{d\theta_{20}}{dy} = K\frac{d\theta_3}{dy} \quad at\ y=0.$$
$$\frac{d\theta_{21}}{dy} = 0 \ at\ y=h=1,\quad \frac{d\theta_{21}}{dy} = 0 \ at\ y=0 \tag{41}$$

Here

$$q_1 = u_1 + iw_1,\ q_{20} = u_{20} + iw_{20},\ q_{21} = u_{21} + iw_{21}, \text{ and } q_3 = u_3 + iw_3. \tag{42}$$

Solutions of equations (31 to 34) and (36 to 39) using boundary conditions (40) and (41) are:

$$\theta_1 = \frac{K+y}{2+K} \tag{43}$$

$$\theta_{20} = \frac{(1+Ky)}{2+K} \tag{44}$$

$$\theta_3 = \frac{(1+y)}{2+K} \tag{45}$$

$$u_{20} = [(d_5 e^{V_1 y} + d_6 e^{-V_1 y})\ cos(V_2 y) + g_7 + g_9 y] \tag{46}$$

$$w_{20} = -[(d_5 e^{V_1 y} - d_6 e^{-V_1 y})\ sin(V_2 y) - g_8 - g_{10} y] \tag{47}$$

$$u_1 = [(d_1 e^{-Ry} + d_2 e^{Ry}) cos(Ry)] \tag{48}$$

$$w_1 = [(d_1 e^{-Ry} - d_2 e^{Ry}) \sin(Ry) + g_1 + g_2 y] \tag{49}$$

$$u_3 = [(d_3 e^{-Ry} + d_4 e^{Ry}) cos(Ry)] \tag{50}$$

$$w_3 = [(d_3 e^{-Ry} - d_4 e^{Ry}) \sin(Ry) + g_3 + g_4 y] \tag{51}$$

$$\begin{aligned}\theta_{21} = {} & \{d_8 y + d_7 + H_{30}e^{2V_1 y} + H_{31}e^{-2V_1 y} + H_{32}\cos(2V_2 y) H_{41} y^4 + H_{42} y^3 + H_{43} y^2 \\ & + H_{33} e^{V_1 y} y \sin(V_2 y) + H_{34} e^{V_1 y} \sin(V_2 y) + H_{35} e^{V_1 y} y \cos(V_2 y) + H_{36} e^{V_1 y} \cos(V_2 y) \\ & + H_{37} e^{-V_1 y} y \sin(V_2 y) + H_{38} e^{-V_1 y} \sin(V_2 y) + H_{39} e^{-V_1 y} y \cos(V_2 y) + H_{40} e^{-V_1 y} \cos(V_2 y)\} \\ & + i\{H_{44} \sin(2V_2 y) + H_{45} e^{V_1 y} y \sin(V_2 y) + H_{46} e^{V_1 y} \sin(V_2 y) + H_{47} e^{V_1 y} y \cos(V_2 y)\} \\ & + i\{H_{48} e^{V_1 y} \cos(V_2 y) + H_{49} e^{-V_1 y} y \sin(V_2 y)) + H_{50} e^{-V_1 y} \sin(V_2 y)\} \\ & + i\{H_{51} e^{-V_1 y} y \cos(V_2 y) + H_{52} e^{-V_1 y} \cos(V_2 y)\}\end{aligned} \tag{52}$$

$$\begin{aligned}u_{21} = {} & (d_9 e^{V_1 y} + d_{10} e^{-V_1 y}) \cos(V_2 y) - R_5 e^{2V1y} - R_7 e^{-2V_1 y} + R_{13} y^3 + R_{17} y^4 \\ & + R_{23} \cos(2V_2 y) - R_{32} e^{V_1 y} y \sin(V_2 y) + R_{41} e^{V_1 y} y \cos(V_2 y) - R_{50} \sin(2V_2 y) \\ & + R_{75} + R_{76} y + R_{77} y^2 + R_{78} e^{V_1 y} \cos(V_2 y) + R_{79} e^{V_1 y} \sin(V_2 y) \\ & + R_{80} e^{-V_1 y} \cos(V_2 y) + R_{81} e^{-V_1 y} \sin(V_2 y) + R_{82} e^{-V_1 y} y \cos(V_2 y) \\ & + R_{83} e^{-V_1 y} y \sin(V_2 y) + R_{84} y^2 e^{-V_1 y} \cos(V_2 y) + R_{85} y^2 e^{-V_1 y} \sin(V_2 y)\end{aligned} \tag{53}$$

$$\begin{aligned}w_{21} = {} & (d_{10} e^{-V_1 y} - d_9 e^{V_1 y}) \sin(V_2 y) + R_6 e^{2V_1 y} y + R_8 e^{-2V_1 y} + R_{14} y^3 + R_{18} y^4 \\ & + R_{24} \cos(2V_2 y) + R_{49} \sin(2V_2 y) - R_{58} e^{V_1 y} y \sin(V_2 y) + R_{61} e^{V_1 y} y \cos(V_2 y) \\ & + R_{86} + R_{87} y + R_{88} y^2 + + R_{89} e^{V_1 y} \cos(V_2 y) + R_{90} e^{V_1 y} \sin(V_2 y) \\ & + R_{91} e^{-V_1 y} \cos(V_2 y) + R_{92} e^{-V_1 y} \sin(V_2 y) + R_{93} e^{-V_1 y} y \cos(V_2 y) \\ & + R_{94} e^{-V_1 y} y \sin(V_2 y) + R_{95} y^2 e^{-V_1 y} \cos(V_2 y) + R_{96} y^2 e^{-V_1 y} \sin(V_2 y)\end{aligned} \tag{54}$$

The constants involved in Equation 46 to Equation 54 are not given for conciseness and solved by taking the parameters as (n, Re, b, P) = (1.5, 5, 1 -5). In the Figures 2 to 8, excluding the differing one, all other values are taken from the set (ϕ, h, Gr, R, m, k, K, λ) = (30°, 1, 5, 1, 0.5, 0.5, 1, 2).

In addition to analyze temperature distribution and impact of velocity on fluid flow it is also important to observe the effect of physical properties such as skin friction and Nusselt number.

The skin friction at the upper plate is given by $\left(\frac{du_1}{dy}\right)_{y=2} = \tau_T$ and

The skin friction at the lower plate is given by $\left(\frac{du_3}{dy}\right)_{y=-1} = \tau_B$.

Similarly the rate of heat transfer from the wall to the fluid, knowing the temperature distribution, at the upper plate (q_T) and lower plate (q_B) is given by

$$\left(\frac{d\Theta_1}{dy}\right)_{y=2} = q_T \, , \left(\frac{d\Theta_3}{dy}\right)_{y=-1} = q_B$$

3. Results and Discussion

Fluid flow and heat transfer in three regions in an inclined channel consisting of composite porous and fluid layers is analysed. The impact of porous parameter λ on velocity field is represented in Figures 2(a) and 2(b). It is noticed that as the value of λ increases, both the axial and transverse velocities decrease in all the regions. The velocity fields for region I and region III, which consist of clear viscous fluids, are large compared to the region II, which consists of porous matrix. The porous matrix in region II drags the fluid back on either side of the porous layer. Further it is interesting to note that the minimum of the velocity occurs at the middle of the region II. There are two maxima one each in region I and region II. It is also found that the presence of two fluid layers on either side of the porous layer increases the mass flow rate in the porous medium. This indicates that the porous frame exerts a notable effect on the velocity field. The impact of the rotation parameter R on velocity field is represented in Figures 3(a) and 3(b). It is observed that axial velocity decreases with increased rotation due to the Coriolis force. Also it is noticed that as the rotation parameter R increases in (0, 1.65), the transverse velocity also increases, but decreases beyond the range as R increases. Figures 4(a), 4(b); 5(a) ,5(b) ; 6(a) , 6(b) and 7(a), 7(b) indicate the effect of Grashof number Gr, angle of inclination ϕ, ratio of viscosities m and the ratio of heights h, showing that as the respective parameter values increase both the axial and transverse velocities increase. Further, it is noticed that for all the parameters the graphs are symmetric in region I and III, and the velocity in the porous region is less when compared with viscous layers.

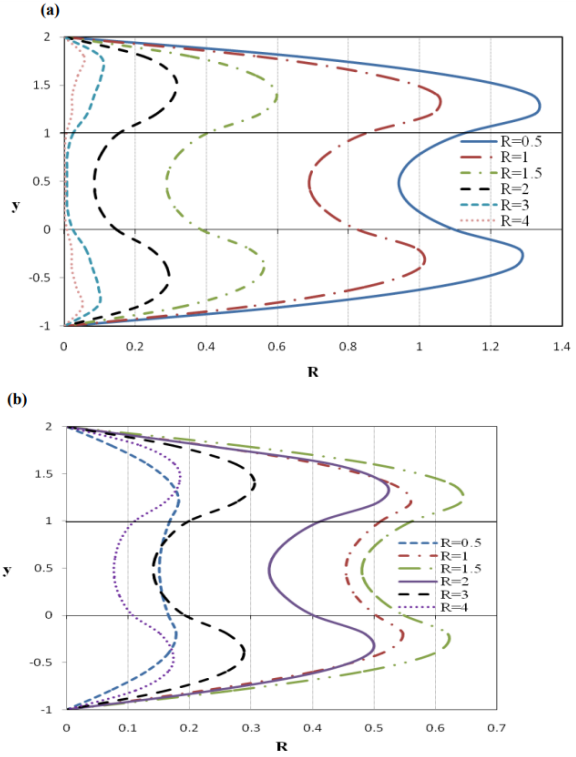

Figure 3. Velocity distribution of R (a) Axial (b) Transvers

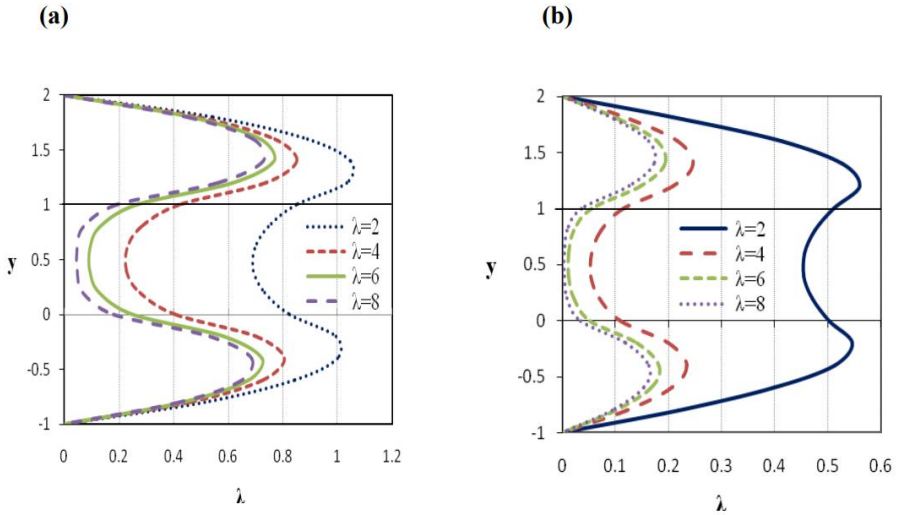

Figure 2. Velocity distribution of λ (a) Axial (b) Transverse

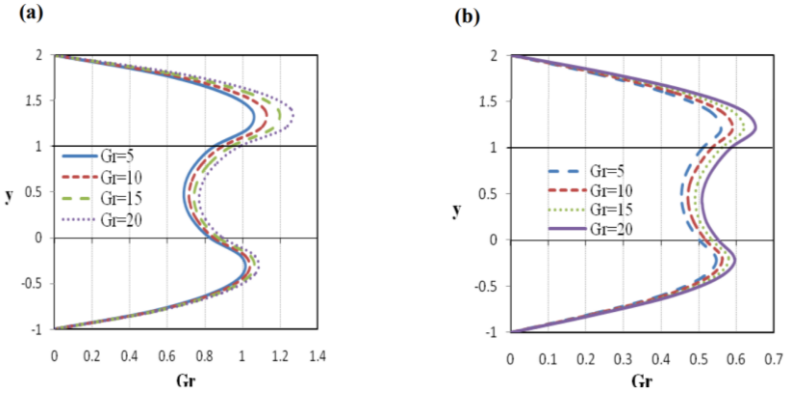

Figure 4. Velocity distribution of Gr (a) Axial (b) Transverse

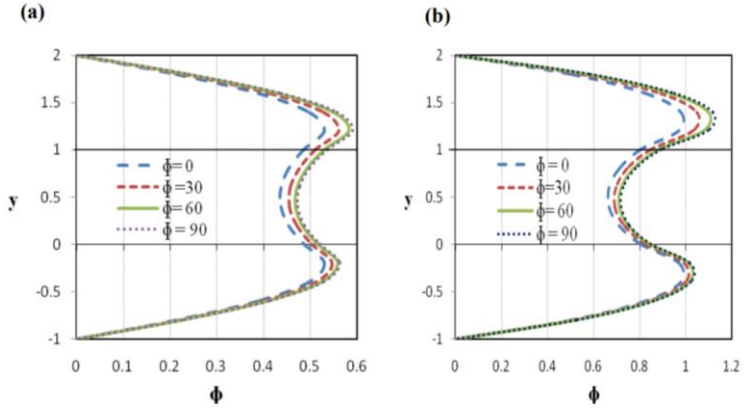

Figure 5. Velocity distribution of ϕ (a) Axial (b) Transverse

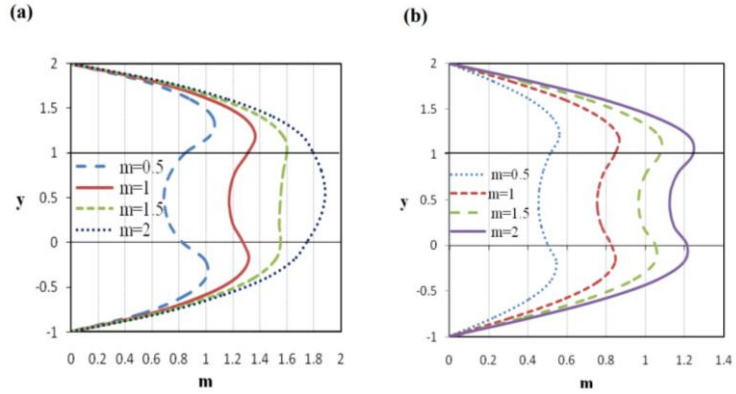

Figure 6. Velocity distribution of m (a) Axial (b) Transverse

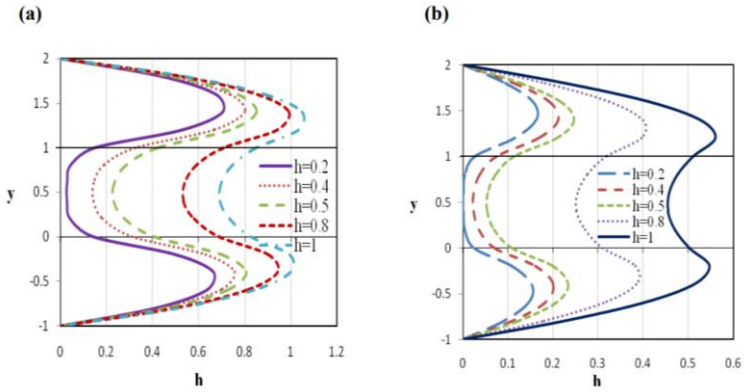

Figure 7. Velocity distribution of h (a) Axial (b) Transverse

Figures 8(a) to 8(f) show the effect of various physical parameters on the temperature field. Temperature profiles are linear for region I and III and non-linear for region II for all governing parameters. Figures 8(a), 8(b) and 8(f) display the effect of porous parameter λ, rotation parameter R and the ratio of heights h on temperature. The increasing values of λ, R and h reduce the temperature in region II. Figures 8(c), 8(d) and 8(e) indicate the effect of Grashof number Gr, angle of inclination ϕ and of ratio of viscosities m showing that as the values of Gr, ϕ and m increase, the temperature increases in region II.

The numerical values of skin friction and Nusselt number are given in Table.1 It is noted that the rate of heat transfer is invariable for upper and lower plates. As the values of parameter λ increase, the skin friction increases for the upper plate and decreases for lower plate. As the value of R increases up to 1.6, the skin friction for the upper and lower plate increases and then decreases. For the parameters Gr, ϕ, m and h, as the values increase the skin friction for upper plate decreases and increases for the lower plate.

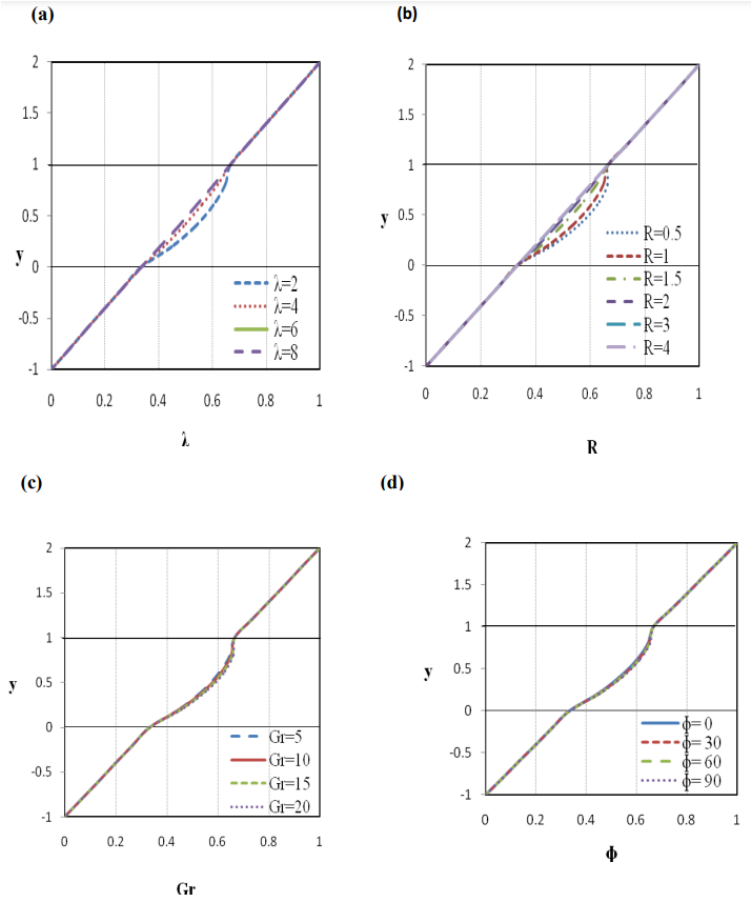

Figure 8(i). Temperature distribution of (a) λ (b) R (c) Gr (d)ϕ

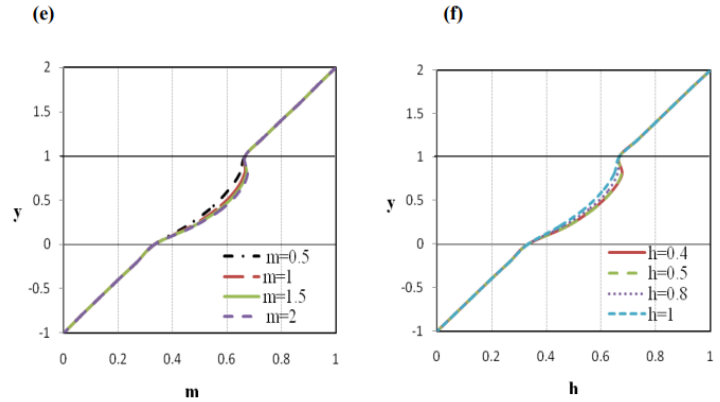

Figure 8(ii). Temperature distribution of (e) m (f) h

Table 1. Skin friction and nusselt number at both upper and lower plates with different physical parameters

Physical parameter	Skin friction at the upper plate (τ_T)	Skin friction at the lower plate (τ_B)	Nusselt number at the upper plate (q_T)	Nusselt number at the lower plate (q_B)
λ = 2	-3.08121	0.607441	0.66667	0.66667
λ = 4	-2.78249	0.372212	0.66667	0.66667
λ = 6	-2.68386	0.288432	0.66667	0.66667
λ = 8	-2.63969	0.250498	0.66667	0.66667
R = 1	-3.08121	0.607441	0.66667	0.66667
R = 1.5	-0.67573	1.606712	0.66667	0.66667
R = 2	-0.21733	1.605959	0.66667	0.66667
R = 3	-0.31824	0.131480	0.66667	0.66667
R = 4	-0.77626	0.048277	0.66667	0.66667
Gr =5	-3.08121	0.607441	0.66667	0.66667
Gr =10	-3.35113	0.617434	0.66667	0.66667
Gr =15	-3.62104	0.627427	0.66667	0.66667
Gr =20	-3.89096	0.637420	0.66667	0.66667
ϕ = 0	-2.81130	0.597448	0.66667	0.66667
ϕ = 30	-3.08121	0.607441	0.66667	0.66667
ϕ = 60	-3.27880	0.614757	0.66667	0.66667
ϕ = 90	-3.35113	0.617434	0.66667	0.66667
m = 0.5	-3.08121	0.607441	0.66667	0.66667
m =1	-3.39093	0.855358	0.66667	0.66667
m = 1.5	-3.58779	1.010610	0.66667	0.66667
m = 2	-3.72364	1.116667	0.66667	0.66667
h = 0.1	-2.56865	0.189271	0.66667	0.66667
h = 0.2	-2.61481	0.229074	0.66667	0.66667
h = 0.4	-2.72173	0.320782	0.66667	0.66667
h = 0.5	-2.78249	0.372212	0.66667	0.66667
h = 0.8	-2.97422	0.527970	0.66667	0.66667

4. Conclusions

It is perceived that the impact of the porous and rotation parameters is to retard the temperature, axial and transverse velocities in three regions. The increase in buoyancy force incorporated through Grashof number and the angle of inclination is to enhance the temperature, axial and transverse velocities for the three layers. The flow and thermal aspects of the fluids in the channel are enhanced by an increase in the ratio of viscosities of the fluids and the ratio of heights of the three regions. The results obtained can be used in heat transfer aspects associated with the multi layer fluids, such as porous or clear or viscous. The applications include both geophysical and industrial fields, such as thermal energy storage system, flow and heat transfer behavior of lubricants in a porous journal bearings and porous rollers, tertiary recovery, groundwater hydrology, reservoir engineering, for purification and filtration processes in chemical engineering, to study seepage of water in river beds, the underground water resources in agriculture engineering, and many others where porous matrix is framed next to a clear fluid.

References

Armaghani, T., Kasaeipoor, A., Alavi, N., & Rashidi, M. M. (2016). Numerical investigation of water-alumina nanofluid natural convection heat transfer and entropy generation in a baffled L-shaped cavity. *Journal of Molecular Liquids, 223*, 243-251. doi:10.1016/j.molliq.2016.07.103

Bian, W., Vasseur, P., Bilgen, E., & Meng, F. (1996). Effect of an electromagnetic field on natural convection in an inclined porous layer. *International Journal of Heat and Fluid Flow, 17*(1), 36-44.

Chauhan, D. S., & Rema, J. (2005). Three-dimensional MHD steady flow of a viscous incompressible fluid over a highly porous layer. *Modelling, Measurement and Control B, 74*, 19-34.

Chauhan, D. S., & Rastogi, P. (2009). Hall current and heat transfer effects on MHD flow in a channel partially filled with a porous medium in a rotating system. *Turkish Journal of Engineering and Environmental Sciences, 33*(3), 167-184. doi:10.3906/muh-0905-6

Constantin, F., Dumitru, V., & Zeeshan, A. (2021). Analytical solutions for two mixed initial-boundary value problems corresponding to unsteady motions of maxwell fluids through a porous plate channel. *Mathematical Problems in Engineering, 2021*, 1-13. doi:10.1155/2021/5539007

Hadidi, N., & Bennacer, R. (2016). Three dimensional double diffusive natural convection across a cubical enclosure partially filled by vertical porous layer. *International Journal of Thermal Sciences, 101*,143-157.

Houman, B., Zeeshan.A., Kavikumar. J., Hajizadeh, A., & Bhatti, B. B. (2020). Numerical modelling for nanoparticle thermal migration with effects of shape of particles and magnetic field inside a porous enclosure. *Iranian Journal of Science and Technology, Transactions of Mechanical Engineering*. doi:10.1007/s40997-020-00354-9

Karuna Sree, C., Paramsetti, S. R. M., & SobhanBabu, K. (2020). Convective two-layered flow and temperature distribution through an inclined porous

medium in a rotating system. *Songklanakarin Journal of Science and Technology, 42*(2), 371-382.

Lu, D. C., Farooq, U., Hayat, T., Rashidi, M. M., & Ramzan, M. (2018). Computational analysis of three layer fluid model including a nanomaterial layer. *International Journal of Heat and Mass Transfer, 122*, 222–228.

Malashetty, M. S., Umavathi, J. C., & Kumar, J. P. (2001). Convective flow and heat transfer in an inclined composite porous medium. *Journal of Porous Medium*, *4*, 15-22.

Malashetty, M. S., Umavathi. J. C., & Pratapkumar, J. (2004). Two fluid flow and heat transfer in an inclined channel containing porous and fluid layer. *Heat and Mass Transfer, 40*(11), 871-876.

Malashetty, M. S., Umavathi. J. C., & Pratapkumar, J. (2005). Flow and heat transfer in an inclined channel containing a fluid layer sandwiched between two porous layers. *Journal of Porous Media*, *8*(5), 443-453.

Rashidi, M. M., Rahimzadeh, N., Ferdows, M., Jashim, U., Md., & Anwar Beg, O. (2012). Group theory and differential transform analysis of mixed convective heat and mass transfer from a horizontal surface with chemical reaction effects. *Chemical Engineering* Communications, *199*(8), 1012-1043.

Rasul, M., & Rashidi, M. M. (2017). Numerical simulation of natural convection heat transfer of a nanofluid in an L-shaped enclosure with a heating obstacle. *Journal of the Taiwan Institute of Chemical Engineers, 72*, 70-84.

Rasul, M., & Rashhidi, M. M. (2018). Forced convection of nanofluids in an extended surfaces channel using lattice Boltzmann method. *International Journal of Heat and Mass Transfer, 117*, 1291-1303.

Riaz, A., Zeeshan, A., Bhatti, M. M., & Ellahi, R. (2019). Peristaltic propulsion of Jeffrey nano-liquid and heat transfer through a symmetrical duct with moving walls in a porous medium. *Physica A.* doi:10. 1016/j.physa.2019.123788.

Riaz, A., Salah, U. K., Zeeshan, A., Sami, U. K., Mohsan, H., & Taser, M. (2020). Thermal analysis of peristaltic flow of nanosized particles within a curved channel with second-order partial slip and porous medium. *Journal of Thermal Analysis and Calorimetry, 143*, 1997–2009. doi:10.1007/s10973-020-09454-9

Sadegh, K., Hossein, T., Arezoo, K., & Rashidi, M. M. (2015). Unsteady convective heat and mass transfer in pseudo plastic nanofluid over a stretching wall. *Advanced Powder Technology, 26*(5), 1319-1326.

Sheikholeslami, M., & Ganji, D.D. (2014). Three dimensional heat and mass transfer in a rotating system using nanofluid. *Powder Technology, 253*, 789–796.

Simon, D., & Shagaiya, Y. D. (2013). Convective flow of two immiscible fluids and heat transfer with porous along an inclined channel with pressure gradient. *Research Inventy: International Journal of Engineering and Science, 2*(4), 12-18.

Sri Ramachandra Murty, P., & Balaji Prakash, G. (2016). Magneto hydrodynamic two-fluid flow and heat transfer in an inclined channel containing porous and fluid layers in a rotating system, *Maejo International Journalof Science and Technology, 10(1),* 25-40.

Sri Ramachandra Murty, P., Balaji Prakash, G., & Karuna Sree, C. (2018). Rotating hydro magnetic two-fluid convective flow and temperature distribution in an inclined channel. *International Journal of Engineering and Technology, 7(4.10) (2018)* 629-635.

Umavathi J. C., Chamkha Ali J., Manjula M. H., & Al-Mudhaf, A. (2005). Flow and heat transfer of a couple stress fluid sandwiched between viscous fluid layers. *Canadian Journal of Physics*, *83*, 705-720.

Umavathi, J. C., Liu, I. C., Kumar, J. P., & Meera, D. S. (2010). Unsteady flow and transfer of porous media sandwiched between viscous fluids. *Journal of Applied Mathematics and Mechanics, 31*(12), 1497-1516.

Zeeshan, A., Nouman, I., Riaz, A., Ameer, B. M., & Aatef, H. (2020). Flow of nonspherical nanoparticles in electromagnetohydrodynamics of nanofluids through a porous medium between eccentric cylinders. *Journal of Porous Media*, 23(12), 1201-1212. doi:10.1615/JPorMedia.2020024813